Quantum Dot Photon Statistics Measured by Three-Dimensional Particle Tracking

Kevin McHale,* Andrew J. Berglund, and Hideo Mabuchi

Physical Measurement and Control 266-33, California Institute of Technology, Pasadena, California 91125

ABSTRACT

We present an instrument for performing correlation spectroscopy on single fluorescent particles while tracking their Brownian motion in three dimensions using real-time feedback. By tracking CdSe/ZnS quantum dots in water (diffusion coefficient $\sim$ 20 μm^2/s), we make the first measurements of photon antibunching (at $\sim$10 ns) on single fluorophores free in solution and find fluorescence lifetime heterogeneity within a quantum dot sample. In addition, we show that 2-mercaptoethanol suppresses short time-scale intermittency (1 ms to 1 s) in quantum dot fluorescence by reducing time spent in the off-state.

Semiconductor quantum dots (qdots) are among the most popular fluorescent markers for biological imaging.[1–4] The photophysical properties of qdots are fairly complicated; qdot fluorescence exhibits intermittency, or blinking, over a wide range of time scales[5–7] and variability within qdot samples leads to nonuniform fluorescence lifetimes.[8] Single-molecule detection techniques are most often used to study these properties, but they suffer from a major limitation in solution: each detected molecule remains in focus only briefly due to diffusion, so data from many molecules must be combined to generate good statistics. Furthermore, dynamics on time scales longer than the diffusion time are difficult to resolve. As a result, most of what is known about qdot fluorescence comes from surface-immobilized qdots, and these may not accurately reflect behavior in solution.[9]

Progress was recently made studying blinking in aqueous environments using wide-field imaging on qdots immobilized in agarose gel,[9] but the use of a charge-coupled device (CCD) camera limited time resolution and the effect of the agarose on the qdots is unknown. Fluorescence correlation spectroscopy (FCS)[10,11] on freely diffusing qdots provides fast time resolution and has yielded results suggestive of blinking,[12] but diffusive motion dominates the FCS curve. With the apparatus we present in this letter, we track the motion of freely diffusing qdots in three dimensions using real-time feedback and measure FCS curves that are not contaminated by diffusion. We measure photon antibunching[8,13,14] on individual qdots and find variation in the fluorescence

lifetime within a qdot sample, and we characterize the effect of blinking on the FCS curve and study the effect of 2-mercaptoethanol (2ME), a known blinking suppressant,[15] on faster time scales than previously investigated.

Techniques that use feedback to track diffusing particles in two dimensions are somewhat mature: methods using a rotating laser beam for localization[16–19] and piezoelectric actuators have produced nearly shot-noise limited accuracy[20] and are well understood theoretically,[21,22] and methods using a CCD camera for localization and electroosmotic flow for actuation[23,24] have produced scientific results in polymer studies.[25,26] However, two-dimensional tracking requires particles to be confined in the third dimension, and this influences their dynamics.[25]

Tracking in three dimensions is noninvasive but more difficult; axial localization methods have not yet performed well enough to track fast-moving particles. One group has accomplished axial localization by dithering the focal depth of the excitation laser using piezo actuators and demodulating the fluorescence signal.[27,28] This mechanical modulation was limited to low frequencies ($\sim$100 Hz) and demodulation and filtering limited the tracking bandwidth to 3 Hz.[28] Other methods have created an axial intensity gradient by introducing optical aberrations[28] or a misaligned confocal pinhole[29,30] but intensity measurements are subject to low-frequency noise,[31] including fluorescence fluctuations due to the particle's dynamics. To date, such methods have only succeeded in tracking objects that move slowly or lack intrinsic photophysical dynamics.

We have developed an approach to three-dimensional localization using fast optical modulation, illustrated in Figure

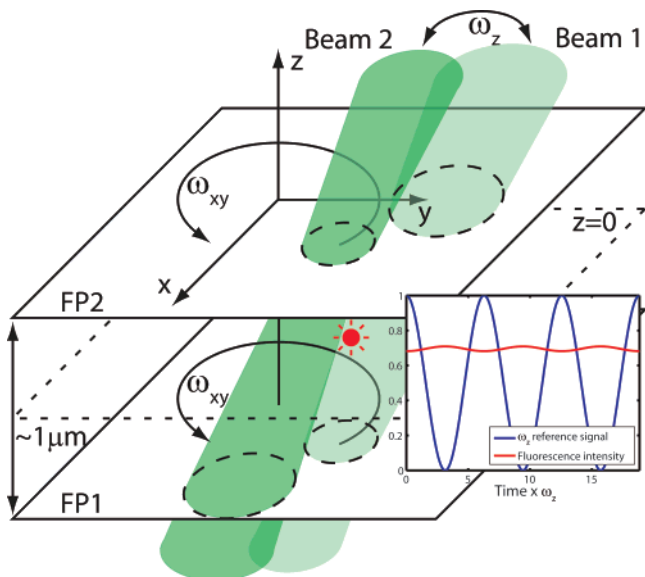* To whom correspondence should be addressed. E-mail: mchale@caltech.edu.

Figure 1. Axial localization scheme as described in the text. Inset shows exaggerated fluorescence intensity fluctuations at frequency ω_z due to the particle's z-position. The z-error signal vanishes in the $z = 0$ plane, so the particle's position is locked there while tracking. FP: focal plane.

Figure 2. Schematic of the experiment. Circled ω_{xy} indicates frequency-modulated (at ω_{xy}) AOM drive signals with a carrier frequency of 40 MHz.

1. Two laser beams rotating at frequency ω_{xy} are focused at different depths inside the sample, separated by about 1 μm, and the total excitation power is alternated between the beams at frequency ω_z. As in two-dimensional tracking,[16−18] the particle's position along x and y is encoded in the magnitude and phase of the ω_{xy} frequency component of the fluorescence signal. The particle's position in z is encoded in the signal in a similar way: the fluorescence intensity is highest when the beam focused nearer to the tracked particle is brightest. As shown in the inset of Figure 1, the ω_z frequency component of the fluorescence signal is either in-phase or 180° out-of-phase with the ω_z drive signal (depending on whether the particle is above or below $z = 0$); the magnitude of the ω_z component is proportional to the particle's distance to the origin. This effect is small (<0.1%) due to the gradual axial variation in the beam intensity but can be measured with a lock-in amplifier. Optical power modulation can be done at high frequencies (>100 kHz) so the demodulated signal bandwidth (~ 1 kHz) is not a limiting factor for tracking small particles. In fact, here we report the first closed-loop tracking of qdots (or comparably small objects) free in solution without the use of viscous agents to slow their motion.

Figure 2 shows the experimental design. A pair of rotating beams is created by first deflecting a 532 nm laser beam along the y-axis at frequency $\omega_{xy} = 2\pi \times 23$ kHz with an acousto-optic modulator (AOM), then splitting the beam and deflecting along the x-axis. The optical powers in the beams are modulated 180° out-of-phase at $\omega_z = 2\pi \times 100$ kHz by attenuating the drive signals into the x-axis AOMs. The beams pass through lens pairs that determine their focal planes in the sample. The beams are combined and focused by a microscope objective (Carl Zeiss, NA 1.2 water immersion) into a 25 μL liquid sample, sandwiched between
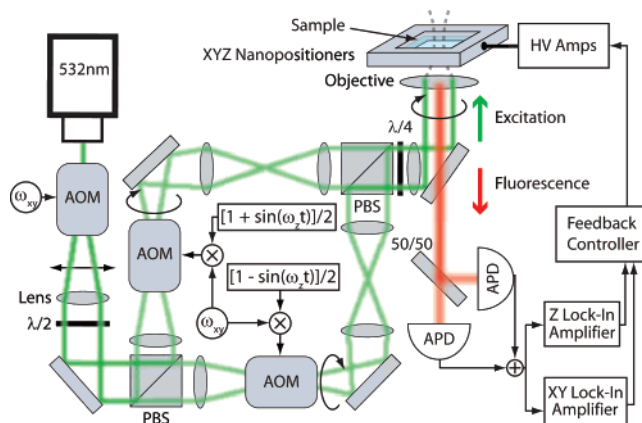
glass coverslides with a separation of ~100 μm. Fluorescence is collected by the objective, separated from the excitation light by a dichroic mirror (Chroma), and measured by a pair of photon-counting avalanche photodiodes (Perkin-Elmer). The fluorescence signal is demodulated by a pair of DSP lock-in amplifiers (Stanford Research Systems), and integrating controllers feed the error signals back to a 100 μm × 100 μm two-axis (x and y) piezo nanopositioner (PI Polytec) that moves the microscope objective and to a 40 μm single-axis (z) piezo (PI Polytec) that moves the sample. A computer records the photon arrival times (with a 79 ns delay between channels) on a time interval analyzer with 75 ps timing resolution (GuideTech) and digitizes the piezo stage positions at a sampling rate of 1 kHz. FCS curves are computed from photon arrival times using an efficient binning algorithm.[32]

Samples consisted of an 80 fM solution of carboxy-derivatized quantum dots (Invitrogen Qdot 655) in 50 mM sodium borate at pH 8.3. For antibunching measurements, 140 mM 2ME was used. For blinking studies the concentration C_{2ME} was varied between 1.4 mM and 140 mM, and 40% v/v glycerol was added to increase solvent viscosity by approximately a factor of 4,[33] improving our ability to track blinking qdots.

Figure 3 shows a sample tracking run. The qdot is tracked for over 20 s, until it reaches the extent of the z-piezo stage. Blinking is evident in the data as the sharp dips in fluorescence intensity near $t = 7$ s and $t = 19$ s. We fit curves to the mean-squared deviations of the stage positions[20,22] to determine the diffusion coefficient, 20.4 ± 2.2 μm^2/s (corresponding to a ~20 nm sphere), and rms localization error, 352 nm along x and y and 272 nm along z, of this particular qdot. We calculate a tracking bandwidth of 51 Hz on the z-axis; this is the fastest axial-tracking bandwidth yet reported.

It is well known that CdSe/ZnS qdots behave as single two-level emitters and their fluorescence exhibits photon antibunching on time scales comparable to the fluorescence lifetime τ_f.[8,14] A nonzero amount of time is needed to cycle the qdot between the ground and excited states, so the probability of detecting two photons simultaneously is zero.
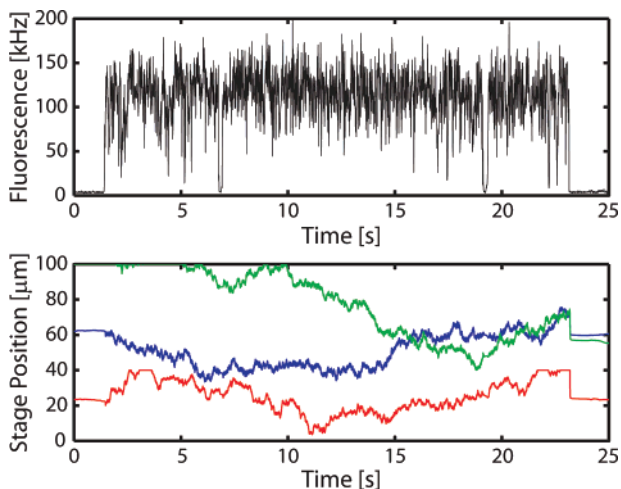
Figure 3. Qdot tracking in 50 mM sodium borate/140 mM 2ME (and no glycerol). Top: fluorescence intensity in 10 ms bins. Bottom: positions of the x- (blue), y- (green), and z- (red) tracking stages. The y-position is initially beyond the range of the data acquisition device.

Figure 4. Rise rates $\Gamma_e + \tau_f^{-1}$ (blue circles) as determined from 80 tracked qdots at varied excitation intensities. Red circles with error bars indicate the sample mean. Insets show $g^2(\tau)$ for data points A and B with fits to eq 1.

This is most clearly measured as subunity pairwise correlation in photon arrival times

$$g^2(\tau) \equiv \frac{\langle f(t, t+\tau)\rangle}{\langle f(t)\rangle^2} = \left\{1 - \alpha e^{-(\Gamma_e + \Gamma_f^{-1})|\tau|}\right\} g_0^2(t) \quad (1)$$

where $f(t_1, t_2)\, dt_1\, dt_2$ is the probability of detecting photons in the intervals $[t_1, t_1 + dt_1]$ and $[t_2, t_2 + dt_2]$; $f(t)\, dt$ is the probability of detecting a single photon in $[t, t + dt]$; the averages are taken over t; Γ_e is the excitation rate, related to the absorption cross section σ, the intensity I and energy hc/λ of incident photons by $\Gamma_e = I\sigma\lambda/hc$; α is the depth of the antibunching dip; and $g_0^2(\tau)$ is the correlation function for all other processes affecting the fluorescence statistics. For an ideal measurement $\alpha = 1$, but background photons and, in the case of qdots, biexcitonic effects[14] both reduce α in real measurements.

In solution, antibunching has been impossible to detect on single fluorophores because typical fluorescence rates are much smaller than τ_f^{-1} so few photons arrive with such short time-spacing during a single fluorophore's diffusion time. We tracked qdots for roughly 3 orders of magnitude longer than than the FCS diffusion time through our laser beam ($\tau_D \approx 26$ ms) with the qdot locked near the peak beam intensity. The resulting $g^2(\tau)$ curves have approximately 100-fold improvements in signal-to-noise, and this was sufficient for measuring antibunching at mean fluorescence rates as low as 65 kHz.

In Figure 4, we show the antibunching rise rates $\Gamma = \Gamma_e + \tau_f^{-1}$ that we measured by fitting eq 1 to data from 80 tracked qdots. The excitation intensity was inferred from the optical power in each beam and the irradiance profiles of the beams as measured on an immobilized fluorescent bead. We estimated a 15% loss in power through the objective, immersion water, and coverslide. The linear fit predicts $\tau_f = 27 \pm 6$ ns, which is comparable to that measured
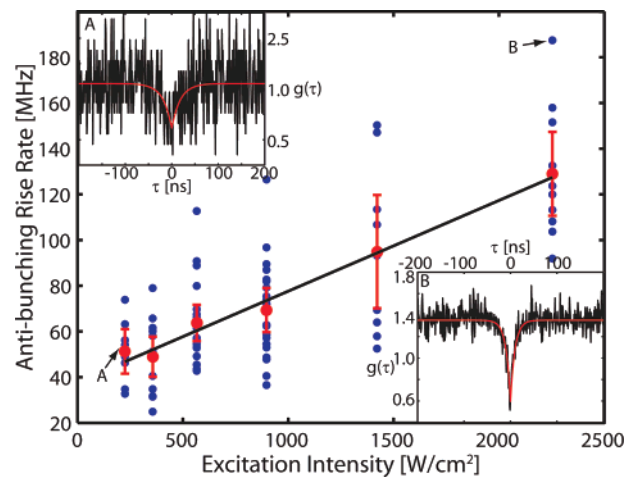
elsewhere,[8] and $\sigma = (1.48 \pm 0.15) \times 10^{-14}$ cm^2. This σ implies a bulk extinction coefficient $\epsilon = N_A\sigma = 8.9 \times 10^6$ M^{-1} cm^{-1}, comparable to the manufacturer's value of 2.1×10^6 M^{-1} cm^{-1}. It is not surprising that we see enhancement in ϵ due to our use of 2ME to suppress blinking, though we cannot be certain that this caused the difference.

The most distinguishing feature of the data is the large spread in Γ observed for different qdots at the same intensity. The relative standard deviation $\Delta\Gamma/\Gamma$ of the rise rate varies little with intensity, ranging between 23 and 40% with a mean of $30 \pm 5\%$. This implies that the spread is not due to poor signal, as the signal-to-noise ratio improves as the intensity increases. It is also not due to intensity fluctuations, as the power in our beam is stable to within 5% over time scales of several hours, which is longer than any of our data runs. As with variation of similar size measured on surface-immobilized qdots,[8] we conclude that the variation we see is primarily due to heterogeneity in the qdot sample; however, we cannot confidently determine the relative contributions of variations in τ_f and σ from our data.

On longer time scales, blinking is a characteristic feature of qdot emission. Because it occurs over time scales extending beyond typical qdot diffusion times, blinking is very difficult to study in solution. For FCS measurements in particular, blinking qdots can easily be mistaken for qdots that do not blink at all because the differences in FCS curves are subtle.[12] Our approach almost eliminates the contribution of diffusion to the FCS curve, and consequently blinking behavior is quite obvious.

In Figure 5, we show FCS curves, each averaged over between 10 and 13 particles, for qdots in 40% v/v glycerol with the excitation intensity fixed at 570 W/cm^2, compared to that for a 60 nm fluorescent bead in water (with approximately the same diffusion coefficient and fluorescence rate). Laser beam rotation causes the oscillations; this and other systematic contributions are described by the formalism we previously developed.[22] The offset as $\tau \to 0$ in the curves for the qdots indicates increased variance in
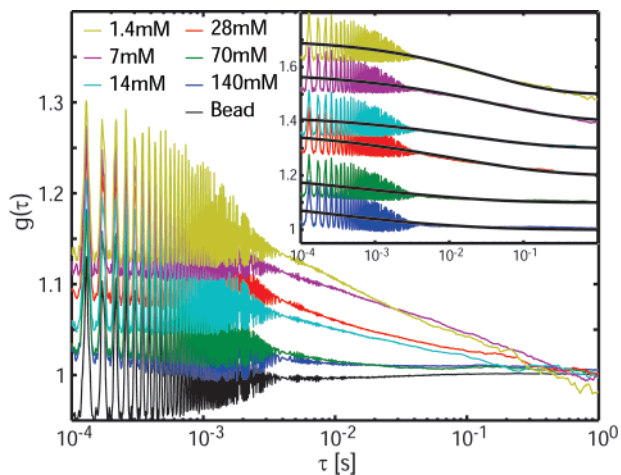
Figure 5. FCS curves for qdots at varied 2ME concentrations, compared to a 60 nm fluorescent bead. The inset shows the qdot curves spaced apart by 0.1 for clarity, with fits to eq 3 shown in black. Fit parameters are given in Table 1.

the fluorescence signal due to blinking. As blinking suppression is decreased, this offset grows, and it decays over a wider range of time scales. We note that all curves have decayed to zero by $\tau \approx 1$ s, indicating that we observe blinking only on shorter times. This is partly because longer off-times are not tolerated by the apparatus: the qdot may move too far while off for it to be detected once it turns on. These $g^2(\tau)$ therefore represent qdot FCS curves conditioned on never switching off for too long. We expect the contribution to our data to be small because we were able to track qdots for long periods at all 2ME concentrations; however, this effect can be eliminated in the future by labeling the qdots with organic dyes,[9] allowing us to probe blinking on even longer time scales.

We model blinking as a jump process between a bright state Φ_1 and a dark state Φ_0 with rates γ_{01} for the $\Phi_1 \rightarrow \Phi_0$ transition and γ_{10} for the $\Phi_0 \rightarrow \Phi_1$ transition. The resulting FCS curve

$$g^2(\tau) = \frac{\gamma_{10} + \gamma_{01}e^{-(\gamma_{01}+\gamma_{10})|\tau|}}{\gamma_{10}} g_0^2(\tau) \qquad (2)$$

provides good fits to the data with strong blinking suppression ($C_{2ME} \geq 70$ mM); however, the steep decay it predicts does not match our observations at lower C_{2ME}. We expect this as qdot blinking is known to exhibit power-law statistics for both on- and off-times.[6,7,9] The complicated nature of these statistics makes explicit calculation of the FCS curve difficult[12] but we find that by introducing a stretching exponent β

$$g^2(\tau) = \frac{\gamma_{10} + \gamma_{01}e^{-[(\gamma_{01}+\gamma_{10})|\tau|]^\beta}}{\gamma_{10}} g_0^2(\tau) \qquad (3)$$

we fit the slower decay quite well. Fits to eq 3 are shown in Figure 5 and fit parameters are given in Table 1. Note that

Table 1. Parameters for Fits in Figure 5

C_{2ME} [mM]	γ_{10} [s^{-1}]	γ_{01} [s^{-1}]	β	$1/(\gamma_{01} + \gamma_{10})$ [ms]
1.4	28	5.7	0.45	30
7.0	23	4.2	0.37	37
14	54	6.7	0.36	16
28	75	13	0.31	11
70	1200	170	0.25	0.73
140	8000	1500	0.2^a	0.11

^{a} For the curve at 140 mM, we had to force $\beta = 0.2$ for convergence of the fit.

$g^2(\tau)$ for $C_{2ME} \geq 70$ mM fits well to both eqs 2 and 3; we show the fits to eq 3 for uniformity, although the steep decays in the data may cause artificially high γ and low β values for these fits. As a result, trends in those values may be exaggerated over these concentrations.

Despite its empirical nature, we chose to leave eq 3 in a form suggestive of eq 2 because the parameters γ_{01} and γ_{10} share some physical relevance in the two equations. In both, $(\gamma_{01} + \gamma_{10})^{-1}$ represents a characteristic time scale of correlation decay and $\gamma_{10}/(\gamma_{01} + \gamma_{10})$ represents the equilibrium probability of the qdot being in Φ_1. At different values of β, however, it is difficult to draw conclusions from different values for the individual γ terms.

The fit parameters in Table 1 confirm some of what is known about 2ME from surface-immobilization studies:[15] we see a trend toward increased total on-time, reflected by increasing offset as $\tau \rightarrow 0$. On time scales longer than 1 s, it was previously shown that this enhancement came from increasing on-times, while the distribution of off-times was unchanged.[15] This is incompatible with the tendency we observe toward shorter correlation times as C_{2ME} increases: the correlation times must *increase* if the on-time increases while the off-time remains constant. Clearly, on these shorter time scales the off-times decrease as C_{2ME} increases. In fact, due to the difficulty in interpreting eq 3 we cannot discount the possibility that the on-times decrease as well; we only know that the off-times must decrease more rapidly.

In addition to providing insight into the behavior of qdots in solution, the results in this letter should serve as a technical benchmark for future real-time tracking experiments. The resolution of dynamics over 9 orders of magnitude in time (antibunching at ~10 ns to diffusion over tens of seconds) on fast-moving qdots is unprecedented even within the closed-loop particle-tracking field. It should be noted that our apparatus is not limited to qdot studies; with the performance reported here it will be possible to track many different types of biological molecules in the future.

References

(1) Bruchez, M. J.; Moronne, M.; Gin, P.; Weiss, S.; Alivisatos, A. P. *Science* **1998**, *281*, 2013−2016.

(2) Chan, W. C.; Nie, S. *Science* **1998**, *281*, 2016−2018.

(3) Larson, D. R.; Zipfel, W. R.; Williams, R. M.; Clark, S. W.; Bruchez, M. P.; Wise, F. W.; Webb, W. W. *Science* **2003**, *300*, 1434−1436.

(4) Michalet, X.; Pinaud, F. F.; Bentolila, L. A.; Tsay, J. M.; Doose, S.; Li, J. J.; Sundaresan, G.; Wu, A. M.; Gambhir, S. S.; Weiss, S. *Science* **2005**, *307*, 538−544.

(5) Nirmal, M.; Dabbousi, B. O.; Bawendi, M. G.; Macklin, J. J.; Trautman, J. K.; Harris, T. D.; Brus, L. E. *Nature* **1996**, *383*, 802−804.

(6) Kuno, M.; Fromm, D. P.; Hamann, H. F.; Gallagher, A.; Nesbitt, D. J. *J. Chem. Phys.* **2000**, *112*, 3117−3120.

(7) Shimizu, K. T.; Neuhauser, R. G.; Leatherdale, C. A.; Empedocles, S. A.; Woo, W. K.; Bawendi, M. G. *Phys. Rev. B* **2001**, *63*, 205316.

(8) Lounis, B.; Bechtel, H. A.; Gerion, D.; Alivisatos, P.; Moerner, W. E. *Chem. Phys. Lett.* **2000**, *329*, 399−404.

(9) Yao, J.; Larson, D. R.; Vishwasrao, H. D.; Zipfel, W. R.; Webb, W. W. *Proc. Natl. Acad. Sci. U.S.A.* **2005**, *102*, 14284−14289.

(10) Elson, E. L.; Magde, D. *Biopolymers* **1974**, *13*, 1−27.

(11) Krichevsky, O.; Bonnet, G. *Rep. Prog. Phys.* **2002**, *65*, 251−297.

(12) Doose, S.; Tsay, J. M.; Pinaud, F.; Weiss, S. *Anal. Chem.* **2005**, *77*, 2235−2242.

(13) Kimble, H. J.; Dagenais, M.; Mandel, L. *Phys. Rev. Lett.* **1977**, *39*, 691−695.

(14) Michler, P.; Imamoglu, A.; Mason, M. D.; Carson, P. J.; Strouse, G. F.; Buratto, S. K. *Nature* **2000**, *406*, 968−970.

(15) Hohng, S.; Ha, T. *J. Am. Chem. Soc.* **2004**, *126*, 1324−1325.

(16) Enderlein, J. *Appl. Phys. B* **2000**, *71*, 773−777.

(17) Levi, V.; Ruan, Q.; Kis-Petikova, K.; Gratton, E. *Biochem. Soc. Trans.* **2003**, *31*, 997−1000.

(18) Berglund, A. J.; Mabuchi, H. *Appl. Phys. B* **2004**, *78*, 653−659.

(19) Berglund, A. J.; Mabuchi, H. *Opt. Express* **2005**, *13*, 8069−8082.

(20) Berglund, A. J.; McHale, K.; Mabuchi, H. *Opt. Lett.* **2007**, *32*, 145−147.

(21) Berglund, A. J.; Mabuchi, H. *Appl. Phys. B* **2006**, *83*, 127−133.

(22) Berglund, A. J.; McHale, K.; Mabuchi, H. *Opt. Express* **2007**, *15*, 7752−7773.

(23) Cohen, A. E.; Moerner, W. E. *Appl. Phys. Lett.* **2005**, *88*, 223901.

(24) Armani, M. D.; Chaudhary, S. V.; Probst, R.; Shapiro, B. *IEEE J. Microelectromech. Syst.* **2006**, *15*, 945−956.

(25) Cohen, A. E.; Moerner, W. E. *Phys. Rev. Lett.* **2007**, *98*, 116001.

(26) Cohen, A. E.; Moerner, W. *Proc. Natl. Acad. Sci. U.S.A.* **2007**, *104*, 12622−12627.

(27) Levi, V.; Ruan, Q.; Gratton, E. *Biophys. J.* **2005**, *88*, 2919−2928.

(28) Ragan, T.; Huang, H.; So, P.; Gratton, E. *J. Fluoresc.* **2006**, *16*, 325−336.

(29) Cang, H.; Wong, C. M.; Xu, C. S.; Rizvi, A. H.; Yang, H. *Appl. Phys. Lett.* **2006**, *88*, 223901.

(30) Cang, H.; Xu, C. S.; Montiel, D.; Yang, H. *Opt. Lett.* **2007**, *88*, 223901.

(31) Bak, P.; Tang, C.; Wiesenfeld, K. *Phys. Rev. Lett.* **1987**, *59*, 381−384.

(32) Laurence, T. A.; Fore, S.; Huser, T. *Opt. Lett.* **2006**, *31*, 829−831.

(33) Shankar, P. N.; Kumar, M. *Proc. R. Soc. London, A* **1994**, *444*, 573−581.

NL0723376